

# A multilevel study on the variation characteristics of tip wake to wind turbines with different fusion tip structures

Weimin Wu<sup>1, 3</sup>, Xiongfei Liu<sup>2</sup>, Wanjun Yan<sup>1,3</sup> and Wenqiang Du<sup>2</sup>

<sup>1</sup>School of Electronic and Information Engineering, Anshun University, Anshun 561000, China;

<sup>2</sup>Yinchuan University of Science and Technology, Yinchuan 750001, China.

<sup>3</sup>The Eastern and Western Innovation Cooperation Joint Laboratory for Aviation Materials and Supporting Industries. Anshun 561000, China;

**Abstract.** Based on the regional division and spatial discretization strategy of the established effective computational fluid dynamics (CFD) numerical model for the wake of an original tip wind turbine blade, a corresponding high-precision CFD calculation model is developed for a series of blade tip wind turbines with different fused tip structures. Transient numerical calculation results are obtained for each base sample matrix corresponding to different geometric parameters of the blade tip. The multi-level proper orthogonal decomposition (POD) mode spatial distribution characteristics of the blade tip vortex wake flow in wind turbines with various fusion tip structures were quantified using a self-developed POD data interface program. This paper analyzes the influence of bending in fusion tip structure on the distribution of vortices at the near-wake region, aiming to find a new and more effective control approach to address full-order flow energy intervention in active flow control.

**Keywords:** Wind turbine wake; proper orthogonal decomposition; blade tip vortex; a series of flow modes.

## 1. Introduction

The wind turbine wake, namely the vortex flow generated behind the wind turbine blade tip during rotation, not only reveals the intricate interaction between the wind turbine and atmospheric conditions but also directly influences its performance and efficiency. As the global demand for sustainable energy continues to grow, wind power, a clean and renewable energy form, has received widespread attention. However, the optimization of wind turbine performance[1] has always been a challenge, and the study of tip vortices is a crucial part of this. The morphology and dynamic characteristics of the wake directly affect the wind energy capture efficiency and operational stability of the wind turbine. By deeply studying the formation mechanism, evolution process, and impact on downstream wind turbine performance of the wake, we can better understand the interaction between wind turbines and the atmospheric environment and provide scientific basis for the design and optimization of wind turbines.

In addition, the study of blade tip wake of wind turbine has important practical application value[2]. In a wind farm, the wake effect between wind turbines will interfere with each other and affect the power generation efficiency of the whole wind farm. By studying wake characteristics, we can optimize the layout of wind farms and the arrangement of wind turbines, reduce wake interference, and improve the overall power generation efficiency of wind farms. This is of great significance for promoting the further development of wind power generation technology and promoting the wide application of clean energy.

Therefore, the present study aims to employ an proper orthogonal decomposition (POD) method[4] within the artificial intelligence algorithm to investigate the flow characteristics of wake behind wind turbines with different fusion tip structures. The purpose of this endeavor is to enhance the understanding of the intricate rotational wake flow field, thereby providing crucial theoretical support and practical guidance for optimizing wind turbine performance and wind farm layout.

## 2. Fusion Tip Structure and Solid Model

### 2.1 Fusion Tip Structure

The wind turbine's fusion tip structure is derived from the design concept of the wing's fusion tip structure found in civil airliners, which effectively enhances aerodynamic performance. By applying this design concept to the wind turbine blade tip structure, we have selected a fusion tip joint located at  $1/6R$  from the leading edge of the blade tip, resulting in a wind turbine blade with a fusion tip structure. The parametric description of this specific type of blade tip structure is illustrated in Figure 1. As no additional structures are incorporated into the blade's tip section and modifications are made solely based on the original design, it is referred to as the fused blade tip structure.

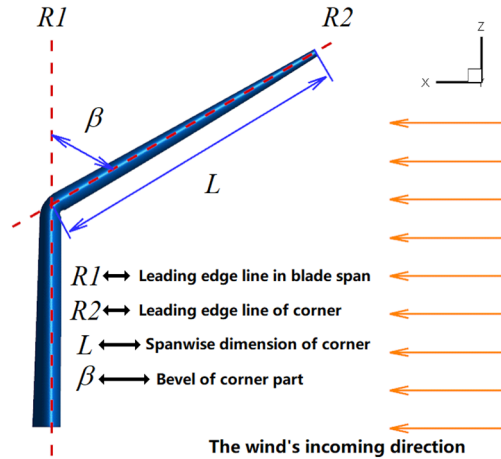


Fig. 1 The parametric characterization of the fused blade tip structure.

### 2.2 Solid Model of Wind Turbine

The wind turbine impeller utilized in this study was designed by the Key Laboratory of Wind Energy and Solar Energy Utilization Technology under the Ministry of Education. It incorporates the Stuttgart Engineering Institute (SERI) series of advanced airfoils specifically developed for wind energy applications, effectively addressing the aerodynamic limitations associated with conventional aviation airfoils. Consequently, it significantly enhances the overall aerodynamic performance of the wind turbine impeller. The essential parameters of the wind turbine impeller are presented in Table 1.

Table 1 The fundamental parameters of the wind turbine impeller

Parameter name	Specific value
Number of blades	3
Blade length	0.7 (m)
Wheel diameter	1.4 (m)
Blade tip chord length	0.04 (m)
Aspect ratio of the span to the average chord length	4.22
Blade tip twist angle	5.8 (deg)
Wind turbine blade airfoil	S series a new airfoil
Rated power	300 (W)
Design wind speed	10 (m/s)
Starting wind speed	3 (m/s)

Due to the unique positioning of the wind turbine blade root, it is subjected to significant alternating bending moments. The stress and strain response of the wind turbine blade root directly impacts the vibration mode of the blade, thereby greatly influencing the overall aerodynamic performance of the wind turbine. Consequently, in consideration of both dynamic performance and issues related to blade and hub assembly, appropriate modifications were made to enhance the design of the blade root. Figure 2 illustrates the corresponding solid models depicting an S-series airfoil wind turbine impeller, improved with enhancements to the fused blade tip.

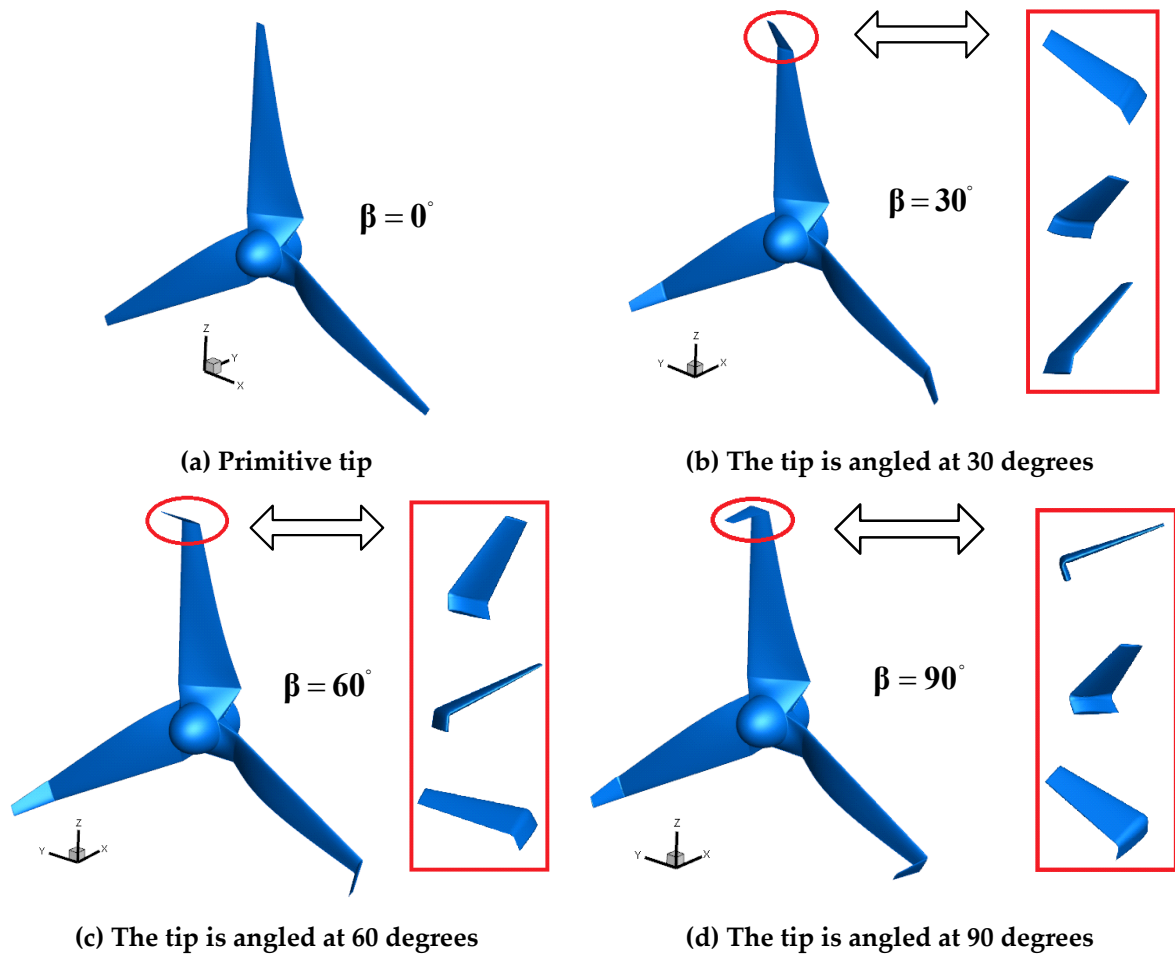


Fig. 2 The wind turbine impellers feature various fusion tip structures.

### 3. The CFD Model for the Tip Region

The calculation area layout, spatial discretization of the grid, and definition of boundary conditions used in this series of CFD models are consistent with the original blade tip wind turbine wake CFD model[5]. Therefore, it is unnecessary to provide detailed explanations here. However, due to differences in the localization of the blade tip structure, a comparison between corresponding localized spatial discretized meshes is presented in Figure 3.

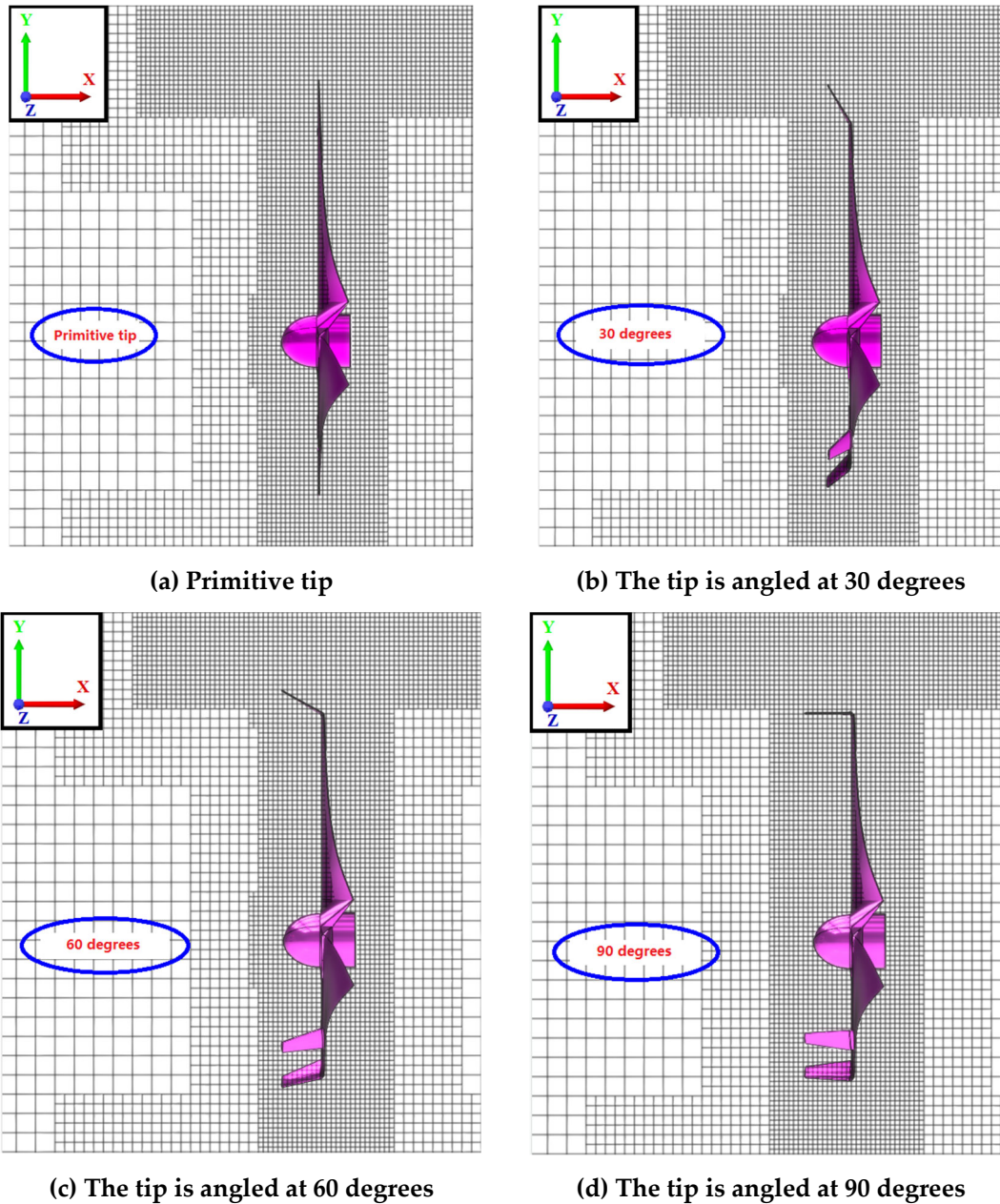


Fig. 3 The comparison of grid localization in calculation models for various fusion tip structures.

The total number of fluid units in the spatial discrete mesh of the aforementioned series of fusion tip structure wind turbine wake CFD models is controlled to be approximately 11 million, ensuring a high computational efficiency while maintaining accurate calculation results.

#### 4. Calculation Results and Analysis with POD Method

The vortex-field physical parameter value corresponding to the calculation results of blade wake flow field in wind turbines with different geometric bevels are selected. The set of initial sample matrices under each bevel state is still based on the same CFD, where the advance time step remains set at  $8.48764 \times 10^{-5}$  s. Simultaneously, consistent selection starts saving the flow field data after the physical propulsion time reaches 6 s and saves snapshot flow field data once every 3 degrees of rotation of the impeller, resulting in a total of 241 snapshots. Additionally, a series of self-developed data structure interface programs are utilized for discrete POD analysis and visual display of corresponding results under different angle geometry parameters.

The spatial distribution characteristics of POD series of blade tip vortices in the local region near the wake of the impeller exhibit noticeable changes when different fusion blade tip structures are

employed. This distinction will be discussed specifically in subsequent sections, focusing on the vorticity fields. To effectively illustrate the alterations in the multi-level features of near-wake localization for the tip vortex, a feature surface that accurately represents changes in the corresponding vortex structure will be defined, as depicted in Figure 4.

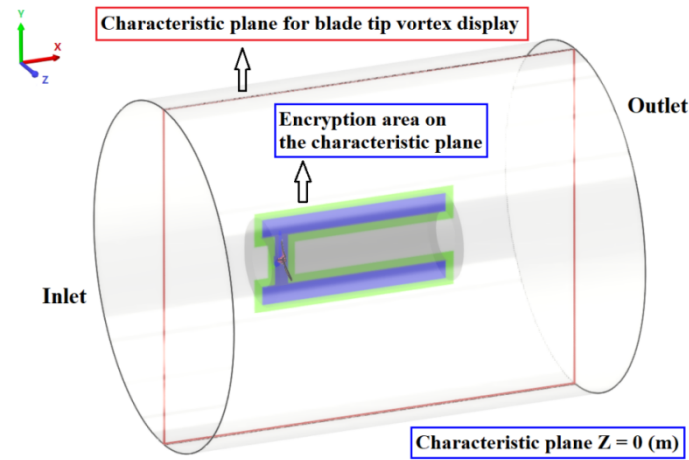
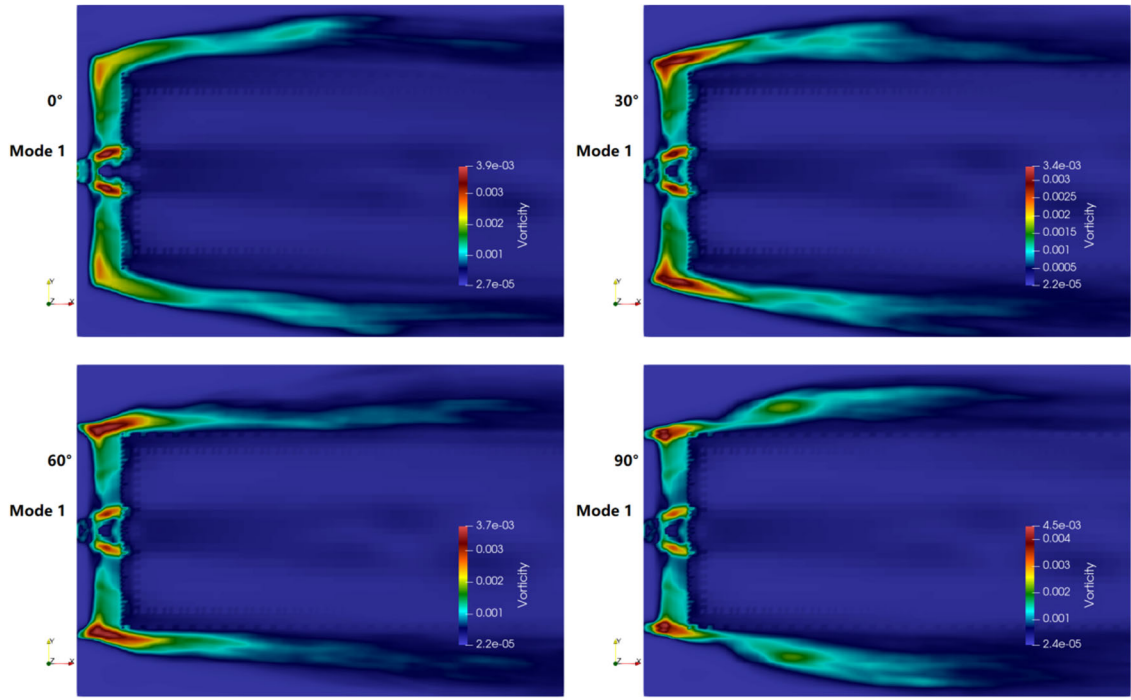


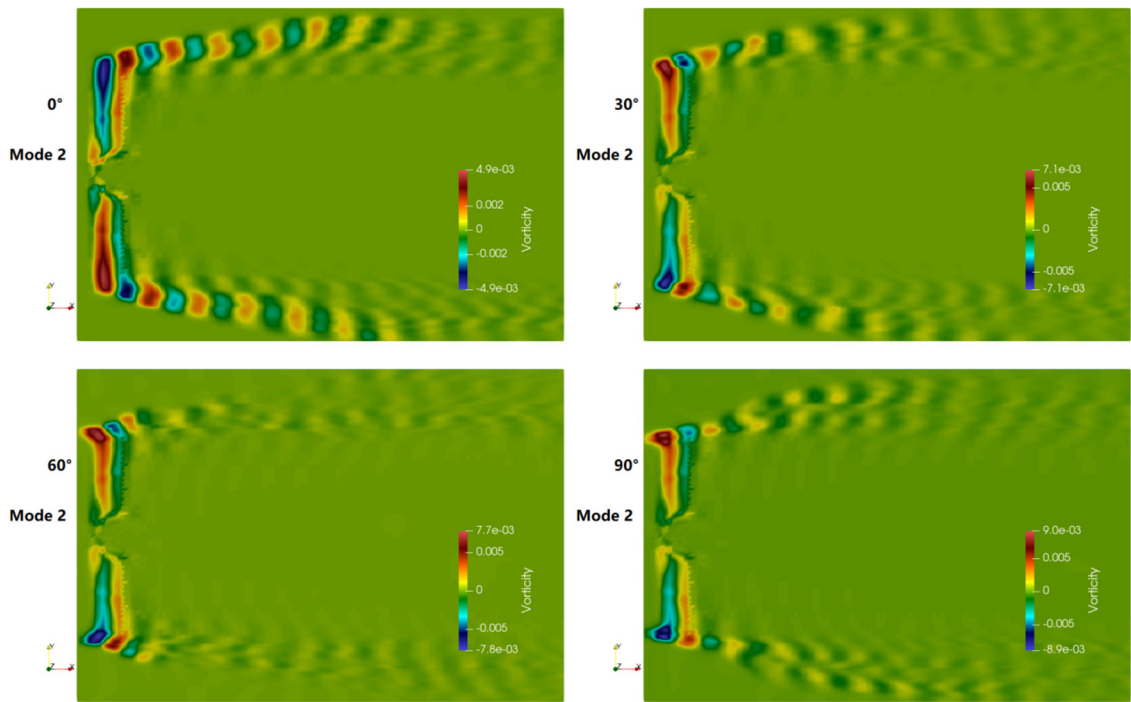
Fig. 4 The spatial distribution of the POD flow mode is represented by the feature surface.

The feature surface of the localized tip-vortex-structure is primarily investigated within the discrete encryption region, while disregarding its influence on changes in the fusion tip structure in the outer far-field region. The subsequent sections separately discuss the corresponding spatial distribution patterns of multi-level POD tip wake localization for a range of physical parameter fields. It should be noted that each order flow mode presented here has been normalized based on their respective physical parameter values to facilitate comparison of characteristic variations within the same order mode.

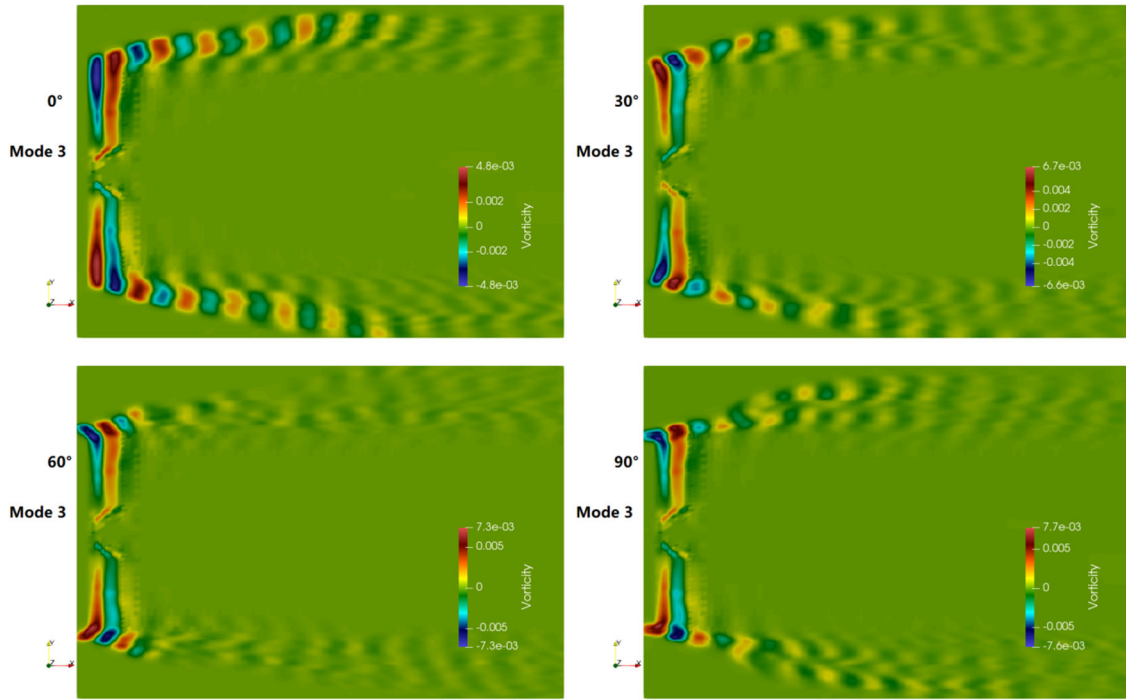
The flow space modes of the tip vortex corresponding to the near-wake vorticity field of the impeller under different fused tip geometry angles are illustrated in Figure 5. The first mode characteristic surface represents the average flow distribution of tip vortices and blade surface attached vortices, as shown in Figure 5(a). As the folding angle increases, the core region of the tip vortex initially expands and then contracts, indicating that the core region with relatively high vortices gradually increases from  $0^\circ$  to  $30^\circ$  to  $60^\circ$ , and then gradually decreases from  $60^\circ$  to  $90^\circ$ . Simultaneously, at a folding angle of  $90^\circ$ , the blade tip exhibits a higher core vorticity value compared to a folding angle of  $0^\circ$ ; furthermore, as the folding angle increases, the center of gravity for blade tip vortex core also moves forward towards downstream direction. The distribution of vorticity along radial direction on blade surfaces also undergoes significant changes with varying folding angles: specifically, radial vorticity is more pronounced on blades subjected to a folding angle of either  $0^\circ$  or  $30^\circ$  compared to those subjected to a folding angle of either  $60^\circ$  or  $90^\circ$ . Additionally, both relative strength and extent range for attached vorticity on central hub surfaces decrease and contract with increasing folding angles, indicating that larger tip angles have an evident inhibitory effect on radial secondary flow over blade surfaces.



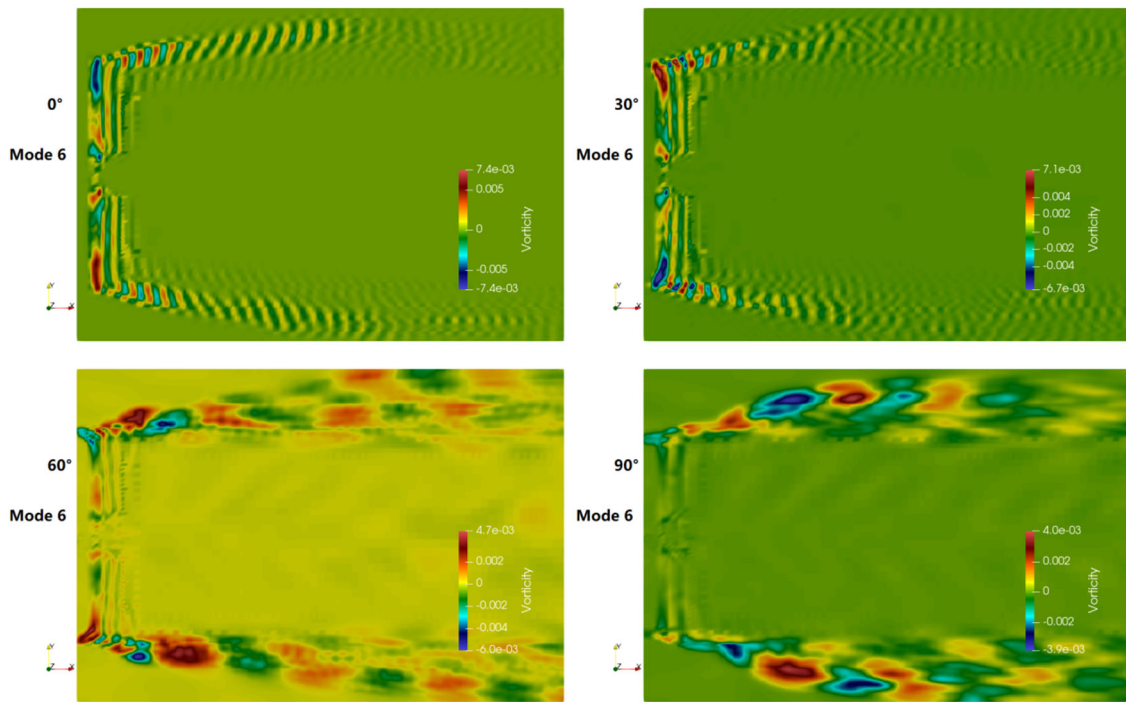
(a) 1st modes



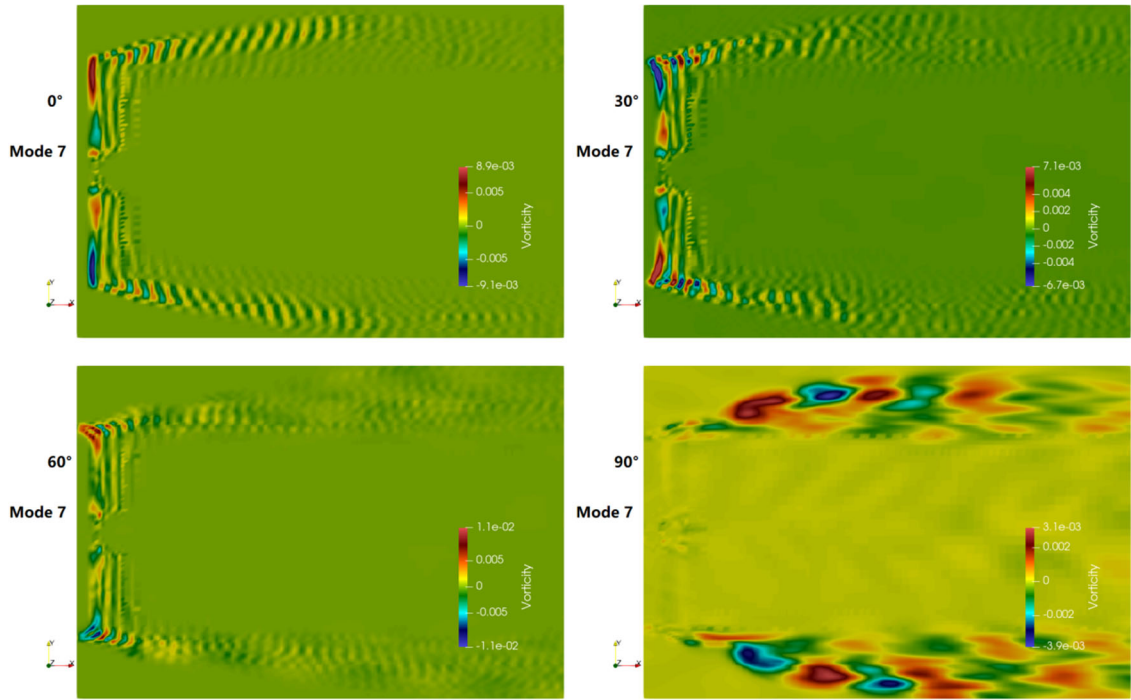
(b) 2nd modes



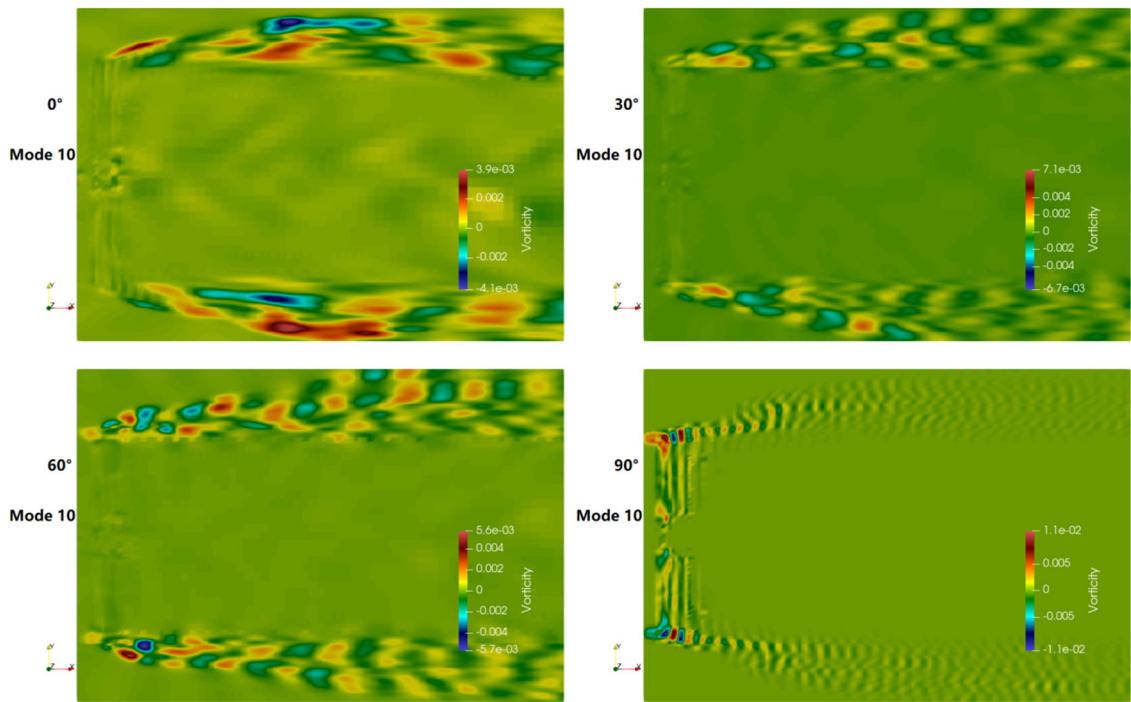
**(c) 3rd modes**



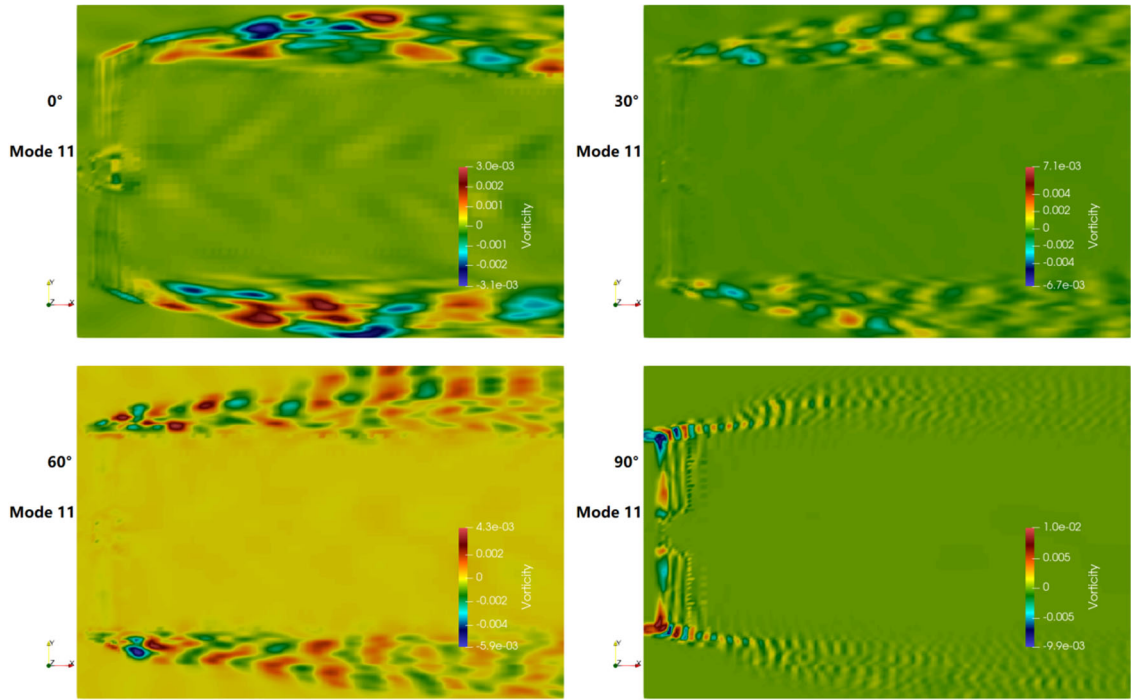
**(d) 6th modes**



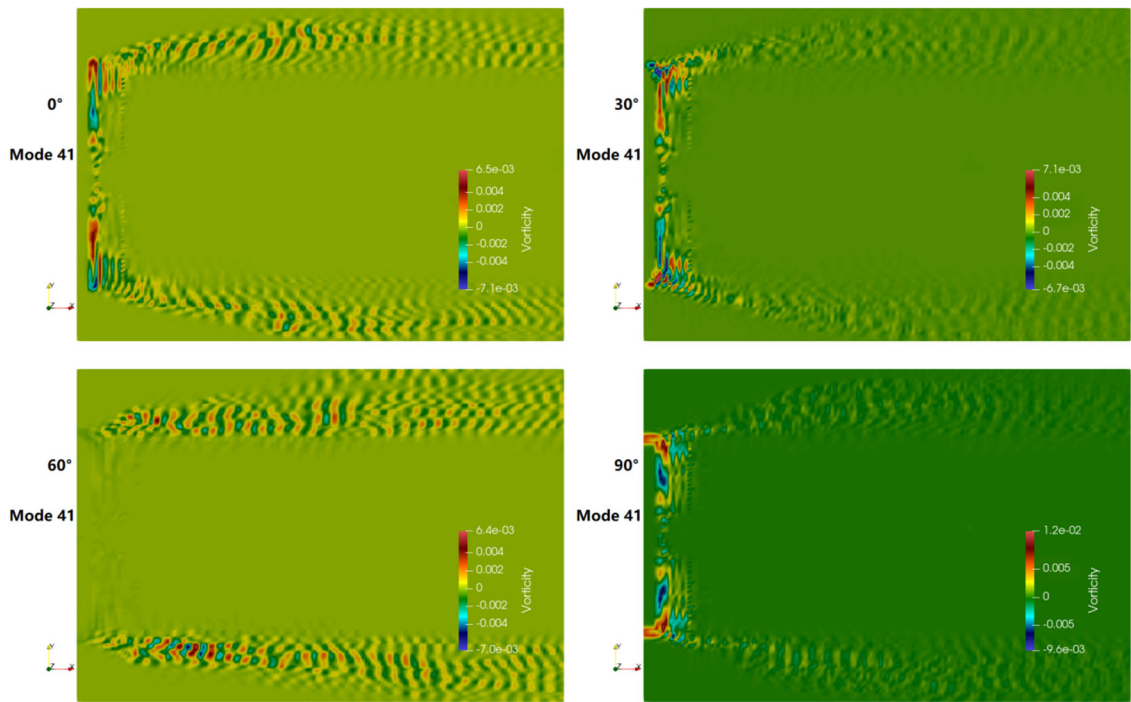
(e) 7th modes



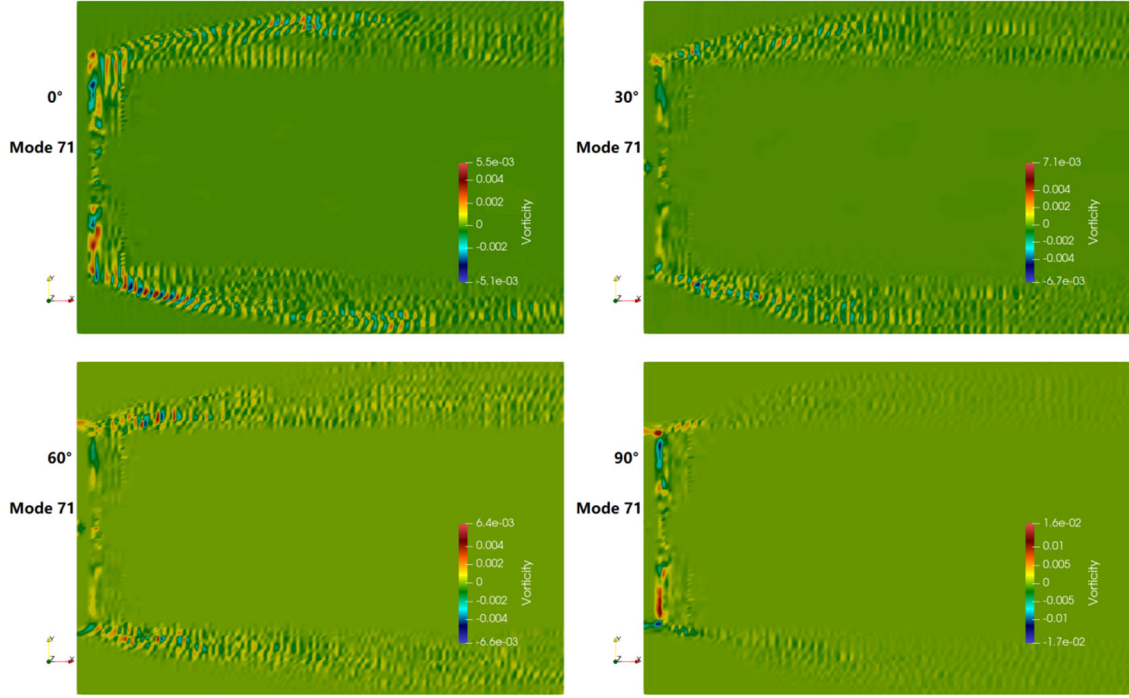
(f) 10th modes



**(g) 11th modes**



**(h) 41th modes**



(i) 71th modes

Fig. 5 The modal characteristics of POD tip flow vorticity are compared among different series with varying folding angles.

The spatial periodic distribution frequency corresponding to the blade tip vortex wake increases with the increase of flow order, as depicted in Figure 5(b) to (c). Additionally, the central region of the initial vortex core exhibits continuous migration characteristics with an increasing fold angle. The radial vorticity on the blade surface and near-wake migration near the blade tip demonstrate similar behavior to that of the first mode. In Figure 5(d), representing the sixth order mode, under both 0 degrees and 30 degrees break angles, there is an increase in spatial distribution frequency for blade tip wake structure with higher orders; however, under a break angle of 60 degrees and 90 degrees, there is a decrease in spatial distribution frequency corresponding to blade tip vortex core near wake while significantly expanding the vortex core region compared to that at 0 degrees and 30 degrees break angles, resulting in a significant reduction in relative high vortex values. This indicates a notable inhibition of shedding frequency for tip vortices and a substantial decrease in vortex-acoustic conversion effect when subjected to large folding angles. As shown in Figure 5(e), representing the seventh mode, its variation characteristics are generally similar to those observed for the sixth mode except that only when reaching a folding angle of 90 degrees can we observe inhibition effects on blade tip angles.

The 10th and 11th order modes are depicted in Figure 5(f) to (g). The POD morphology of the vortex system corresponds to a continuous thinning of the near-wake vortex system due to an increase in blade tip angle, while its periodic spatial distribution frequency continues to rise. This phenomenon can be attributed to the fact that the 10th and 11th modes represent wake modes associated with attached vortices on the blade surface, indicating that the folding structure at the tip significantly influences these wake modes by causing them to thin out further as the fold angle increases.

The 41st and 71st order modes are depicted in Figure 5(h) to (i). These two representative higher-order flow modes correspond to the deep fusion pattern of tip vortices and attached vortices. It is observed that their respective wake vortex core ranges remain relatively unchanged as the tip angle increases. However, under a folding angle of 90 degrees, the radial vortex system on the blade surface exhibits a wider range of relatively high vorticity. This suggests that the corresponding fusion tip structure strongly inhibits secondary flow along the radial blade surface.

## 5. Summary

In the investigation, the Proper Orthogonal Decomposition (POD) method is employed to numerically analyze the near-wake flow corresponding to different fusion blade tips. The spatial distribution characteristics of the POD series of blade tip vortices in the near-wake region of the impeller exhibit significant variations compared to those of the original blade tips due to changes in blade tip angles. Specifically, in both first order and higher modes, there is an initial increase followed by a decrease in the nucleation region of tip vortices with increasing folding angle. Meanwhile, the blade tip's 90-degree folding angle exhibits a relatively higher core vorticity value compared to that of the 0-degree folding angle. Moreover, as the folding angle increases, the center of the blade tip vortex core continuously advances towards the flow direction. The presence of the radial vortex system on the blade surface is more pronounced when subjected to a bend angle of 0° and 30° compared to that under a bend angle of 60° and 90°.

Additionally, the relative strength and core range of the attached vortex on the central hub surface decrease and contract with an increase in the bend angle, indicating that a larger tip bend angle significantly impacts the radial secondary flow on the blade surface. Moreover, under a bend angle of 60° and 90°, there is a decrease in spatial distribution frequency corresponding to the near wake of the tip vortex core, accompanied by a significant enlargement in its region. Furthermore, at high vorticity levels, there is notably lower relative vorticity value than at low vorticity levels under these large folding angles. This suggests that shedding frequency of tip vorticity is considerably inhibited while also experiencing decreased vorticity conversion effects. Notably, when subjected to a bend angle of 60 degrees, suppression in radial displacement for tip wake is most evident; however, within close proximity to this wake at a bend angle of 90 degrees exists an area exhibiting rapid radial displacement.

The research progress and achieved results in this work, along with the corresponding data structure interface program developed, can provide theoretical and technical references for targeted control of important high-order vortices in complex rotating flows. Furthermore, it aims to explore a novel and more effective approach to address the issue of full-order flow energy intervention in active flow control.

## Acknowledgements

The research has been funded by the Eastern and Western Innovation Cooperation Joint Laboratory Project of Aviation Materials and Supporting Industries (No.2024-011), the Chongqing Natural Science Foundation of China (No.cstc2020jcyj-msxmX0314), and the Ningxia Key Research and Development Program of Foreign Science and Technology Cooperation Projects(No.202204).

## References

- [1] Kasmaiee S, Tadjfar M, Kasmaiee S. Optimization of Blowing Jet Performance on Wind Turbine Airfoil under Dynamic Stall Conditions Using Active Machine Learning and Computational Intelligence[J]. *Arabian Journal for Science and Engineering*, 2024, 49(2): 1771-1795.
- [2] Wang L, Dong M, Yang J, et al. Wind Turbine Wakes Modeling and Applications: Past, Present, and Future[J]. *Ocean Engineering*, 2024, 309: 118508.
- [3] Zhang Z, Yang H, Zhao Y, et al. A Novel Wake Control Strategy for a Twin-rotor Floating Wind Turbine: Mitigating Wake Effect[J]. *Energy*, 2024, 287: 129619.
- [4] Zarepour M, Bergstrom D J, Spiteri R J. Identifying Dominant Flow Structures in a Bubbling Gas-particle Fluidized Bed Using the Spectral Proper Orthogonal Decomposition[J]. *Chemical Engineering Science*, 2024, 293: 120048.
- [5] Wu W, Liu X, Yao J, et al. A Multilevel Investigation into Tip Wake of Wind Turbine Using Sirovich-type Proper Orthogonal Decomposition[J]. *International Journal of Multiphysics*, 2024, 18(2s): 96-132.